Multiple morphodynamic equilibria in a one–dimensional tidal embayment

H.M. Schuttelaars and H.E. de Swart

Institute for Marine and Atmospheric Research, Utrecht University,
P.O.Box 80.005, 3508 TA Utrecht, The Netherlands

Abstract

A one–dimensional model describing the possible morphodynamic equilibria for a long tidal embayment is developed and analyzed. The system is driven by a prescribed external M_2 and M_4–tide at the open seaward boundary. Furthermore overtides are generated internally. It is demonstrated by using continuation methods that the model allows for morphologic equilibria characterized by bed profiles that have a prescribed depth at its entrance and a zero water depth at the land–side of the embayment.

If the system is only forced by an externally prescribed M_2–tide, one unique equilibrium is found. If an externally prescribed overtide is forcing the system as well, more than one type of equilibrium can be found. For embayments with lengths smaller than the M_4 frictional length scale, advective fluxes due to internally generated and externally forced overtides make an approximate balance. The effect of bottom friction is small and the tidal motion has the characteristics of a standing wave. The bed can become very deep, up to 7 times the depth at the entrance of the embayment. For longer embayments, *i.e.*, with lengths larger than the M_4 frictional length scale, an approximate balance between internally generated advective fluxes is observed. Bottom friction becomes important and the tide propagates as a travelling wave. The maximum water depth is of the order of twice the depth at the entrance. If the externally prescibed M_4–tide is strong enough, multiple equilibria can be found for embayment lengths near the M_4 frictional length scale. Furthermore, morphodynamic equilibria can only be found for embayments with lengths smaller than the frictional length of the M_2–tide which also depends on the amplitude of the external M_4–tide. For even longer embayments the velocities at the end of the embayment become too small to keep the embayment open.

1 Introduction

In many tidal inlets and estuaries a dynamic interaction between water motions and morphology is observed. This usually results in a complex pattern of channels and shoals, see e.g. the Western Scheldt (Van den Berg *et al.*, 1990). This estuary is located in the the south–west of Holland and Belgium and serves as the main navigation lane to the harbour of Antwerp. In the Western Scheldt economical and ecological interests often interfere. For shipping purposes it would be advantageous if the channel was canalized On the other hand, the Western Scheldt has important feeding grounds for birds and other animals for which the system has to be kept as dynamic as possible. To keep the harbour open for large ships, the navigation lane of the Western Scheldt has to be dredged continuously ($8 \cdot 10^6\,\mathrm{m}^3\mathrm{year}^{-1}$) (Verbeek *et al.*, 1998). Since the morphology is also very sensitive to changes in exogeneous conditions (see Van der Spek (1997)) our understanding of the estuarine processes must be deepened to be able to manage and control the changes in these complex systems. Therefore, a two–dimensional global model of a tidal embayment will be developed in which only the basic physical processes responsible for the observed phenomena are retained.

In this paper the analysis will be restricted to a one–dimensional model, since this provides the information necessary to perform a two–dimensional analysis resulting in channel–shoal behaviour (see Schuttelaars (1997, to appear)). In this paper the existence of possible morphodynamic equilibria and the important physical processes will be studied.

Important generalizations with respect to Schuttelaars & De Swart (1996), in which a short embayment was studied, are the spatial variations of both the vertical and horizontal tide due to advective and frictional effects. Furthermore, in a long channel the net transport of suspended sediment is mainly due to advection, whereas in a short embayment the main transport mechanism is diffusive transport. Important differences with De Jong (1998) are the negligence of river influence and the incorporation of diffusive boundary layers in the averaged concentration equation.

In section 2 the model will be presented, in section 3 the equations are scaled and analyzed using an asymptotic method. In section 4 morphodynamic equilibria and their characteristics will be studied. In the last section some conclusions and suggestions for future work will be made.

2 Model Description

The embayment under study is a rectangular basin. If for a short embayment it is assumed that the waterdepth becomes zero at the landward end, the equilibrium bed profiles obtained are such that a spatially uniform shear stress distribution is attained, which seems to be consistent with field observations (Friedrichs, 1995). Moreover, the relation between cross–sectional area and the tidal prism appears to be linear as data indicate (De Vriend, 1996).

Motivated by these results, it is hypothesized that that in case of a long embayment the influence of the river inflow is not present or can be neglected. This assumption leads to an embayment that has a zero water depth at the landward end. The width is much smaller than both the length of the embayment and the Rossby deformation radius, which permits to model the embayment as one–dimensional (no variations in the cross–channel direction). The system is forced with an externally prescribed vertical tidal elevation ζ with respect to the undisturbed water depth at the entrance. Note that due to surface elevations the boundary at the end of the embayment is a *moving* boundary (see

Fig. 1, where the length, corresponding to sea level ζ_1 and ζ_2 is denoted by L_1 and L_2, respectively). The reference water depth is denoted by H, the bed elevation by h and u

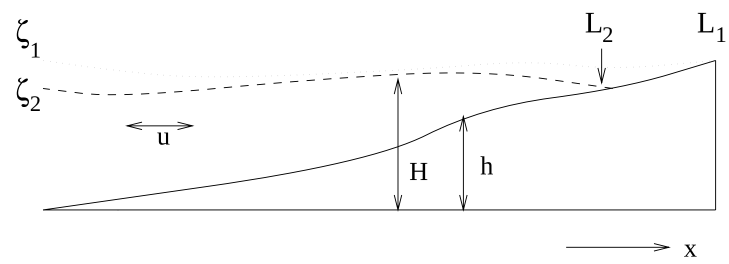

Figure 1: Cross–sectional view of the embayment.

denotes the horizontal tide.

The water motions are decribed by the depth–averaged shallow water equations for a homogeneous fluid (Csanady, 1982). The bottom friction in the momentum equation is linearized (see Lorentz (1922); Zimmerman (1982, 1992)). At the open boundary the tidal elevation ζ is prescribed. At the closed end, the kinematic boundary condition is used.

The sediment in the embayment consists of noncohesive material with only one grain size and is mainly transported as suspended load. This transport is described by a depth–integrated concentration equation (see Van Rijn (1993)). The boundary condition for the concentration equation is that the net sediment flux at the average position of the moving boundary is zero. At the entrance it is imposed that the bed does not change. Since the bed only changes due to tidally averaged erosion and deposition, additional boundary conditions are needed. We therefore require that no diffusive boundary layer in the time–varying concentration develops at the entrance of the embayment.

The bottom evolution equation is derived from continuity of mass in the sediment layer. An initial condition must be supplied. Since at $x = 0$ the total deposition equals the erosion, the bed remains fixed at $x = 0$, at the end the water depth is always zero.

3 Scaling and Expansion

The equations as proposed in section 2 are scaled using

$$x = L\tilde{x}, t = \tilde{t}\sigma^{-1}, u = \frac{A\sigma L}{H}\tilde{u}$$
$$\zeta = A\tilde{\zeta}, h = H\tilde{h}, C = \frac{\alpha U^2}{\gamma}\tilde{C} \qquad (1)$$

Here L is chosen such that $x = 1$ is the intersection point of the bed profile and the undisturbed water level. The radian frequency of the main tidal constituent is denoted by σ and A is the amplitude of the vertical tide at the entrance. Suppressing the tilde, the equations read

$$\zeta_t + [(1-h+\epsilon\zeta)u]_x = 0 \tag{2a}$$

$$u_t + \epsilon u u_x + \lambda_{\mathrm{L}}^{-2}\zeta_x + r\frac{u}{1-\alpha(h-\epsilon\zeta)} = 0 \tag{2b}$$

$$a\left[C_t + (\epsilon u C - \mu C_x)_x\right] = u^2 - C \tag{2c}$$

$$h_\tau = -\left\langle u^2 - C\right\rangle \tag{2d}$$

Here ϵ is, apart from a factor of 2π, the ratio of the tidal excursion (the distance travelled by a fluid particle in a tidal period) and the tidal inlet length (for the definitions of the nondimensional parameters in the model, see table 1). The constant $\lambda_{\mathrm{L}}(= 2\pi\sqrt{gH}/\sigma)$

Parameters in the nondimensional model

$\epsilon = \frac{A}{H} = \frac{U}{\sigma L}$	$\lambda_{\mathrm{L}} = \frac{2\pi L}{L_{\mathrm{g}}}$	$r = 8C_{\mathrm{D}}AL/(3\pi H^2)$
$a = \frac{\sigma}{\gamma}$	$\mu = \frac{\mu_\star}{\sigma L^2}$	$\delta_{\mathrm{s}} = \frac{\alpha U^2}{\rho_{\mathrm{s}}(1-p)H\sigma}$

Table 1: Parameter definitions in the nondimensional model.

is the ratio of the frictionless tidal wave length L_{g} and the embayment length, and r is a measure for the frictional strength which depends on the drag coefficient C_{D}. The parameter α in the bottom friction is used to vary the influence of the depth on the friction; since $1-h+\epsilon\zeta$ becomes zero at the end of the embayment, this term would become infinite, which is not a very realistic parameterization of the bed friction. Since the friction becomes large but finite when the water depth becomes small, α is chosen to be close to 1.

Furthermore, a is the ratio of the timescale of the deposition process and the tidal period and μ is the ratio of the tidal period and the diffusive time scale. Here $\tau = \delta_{\mathrm{s}} t$ is a slow time coordinate and δ_{s} is the ratio of the tidal period and the morphological timescale.

The boundary conditions at the entrance $x = 0$ are

$$\zeta = \cos(t) + \beta\cos(2t-\phi) \tag{3a}$$

$$h = 0 \tag{3b}$$

$$C'(x,t,\mu) = C'(x,t,\mu=0) \tag{3c}$$

where C' is the oscillatory part of the concentration equation. Here β is the ratio of the M_4 amplitude and the M_2 amplitude at the entrance, ϕ is the phase difference between the M_4 and M_2 tidal constituents at this location, defined by $\phi = \phi_{M_4} - 2\phi_{M_2}$. At the closed end the boundary conditions read

$$u_x \quad \text{is finite} \tag{4a}$$

$$\langle \epsilon u C - \mu C_x\rangle = 0 \tag{4b}$$

$$C'(x,t,\mu) = C'(x,t,\mu=0) \tag{4c}$$

The first boundary condition is the kinematic boundary condition, the second one states that no net sediment flux is allowed through $x = 1$. The boundary condition for the time–varying concentration states that no diffusive boundary layers develop near the entrance and the end of the embayment in the oscillatory part of the concentration.

These equations will be solved by making an expansion with respect to the small parameters ϵ and β, up to first order. No assumption on the ratio of ϵ and β is made. It is only assumed that $\beta \ll 1$, *i.e.* that the amplitude of the M_2 constituent is much stronger than that of the externally prescribed M_4 constituent. Hence for the water elevation ζ the following expansion is made:

$$\zeta = \zeta_0 + \epsilon\zeta_1 + \beta\zeta_{o,1} \dots \tag{5}$$

with

$$\zeta_0 = \zeta^{\mathrm{s}} \sin(t) + \zeta^{\mathrm{c}} \cos(t) \qquad \zeta_1 = \zeta^0 + \zeta^{2\mathrm{s}} \sin(2t) + \zeta^{2\mathrm{c}} \cos(2t)$$
$$\zeta_{o,1} = \zeta_{\mathrm{o}}^{2\mathrm{s}} \sin(2t) + \zeta_{\mathrm{o}}^{2\mathrm{s}} \cos(2t)$$

Here ζ_0 decribes the main tidal constituent and ζ^0 the mean water level which is forced by net transfer of momentum induced by the tidal wave. Furthermore $\zeta^{2\mathrm{c}}, \zeta^{2\mathrm{s}}$ are the components of the internally generated M_4–overtide and $\zeta_{\mathrm{o}}^{2\mathrm{s}}, \zeta_{\mathrm{o}}^{2\mathrm{c}}$ those of the M_4–overtide generated by external forcing. Similar expansions for u and C are made. The same notation is used as in the above expansion (use of superscripts to describe the temporal behaviour on the short time scale and the subscripts to make a distinction between internally generated and externally driven quantities). Of course, one can write $\zeta_0 = |\zeta_0| \cos(t - \phi_{\zeta_0})$, etc., as well. Here $|\zeta_0|$ is the amplitude of the M_2 vertical tidal elevation, ϕ_{ζ_0} its phase angle.

If a bed profile and the surface elevations at the entrance of the embayment are given, the horizontal and vertical velocities and the concentration can be calculated explicitely. This information is used to calculate a net sediment flux F and to rewrite the bed evolution equation as

$$h_\tau = -F_x(h, h_x, h_{xx}) \tag{6}$$

Hence the bed changes due to divergences or convergences of the tidally averaged sediment flux F. From eqn. (6) it is clear that an equilibrium bed profile is found if $h_\tau = 0$. Using the boundary conditions on the sediment flux, eqn. (4b), this means that in equilibrium the net sediment flux throughout the embayment has to be zero. After expanding the flux in the small parameters ϵ and β, this condition reads

$$\begin{aligned} F = -a\mu C_x^0 + a\epsilon^2 \left(u^0 C^0 + \frac{1}{2} \left[u^{\mathrm{s}} C^{\mathrm{s}} + u^{\mathrm{c}} C^{\mathrm{c}} + u^{2\mathrm{s}} C^{2\mathrm{s}} + u^{2\mathrm{c}} C^{2\mathrm{c}} \right] \right) \\ + a\frac{1}{2}\epsilon\beta \left(u^{\mathrm{s}} C_{\mathrm{o}}^{\mathrm{s}} + u^{\mathrm{c}} C_{\mathrm{o}}^{\mathrm{c}} + u_{\mathrm{o}}^{2\mathrm{s}} C^{2\mathrm{s}} + u_{\mathrm{o}}^{2\mathrm{c}} C^{2\mathrm{c}} \right) = 0 \end{aligned} \tag{7}$$

Note that this flux consists of three main parts. The first is due to diffusive sediment transport and is proportional to $a\mu$. The second part is proportional to $a\epsilon^2$ and describes a flux due to internally generated overtides. The final part, which is proportional to $a\epsilon\beta$, are fluxes induced by the presence of externally prescribed overtides. So if an equilibrium bed profile is found, the combination of the velocity and concentration fields

Quantities in the model		
$H = 15$ m	$A = 1.5$ m	$\sigma \sim 1.4 \cdot 10^{-4}$ s^{-1}
$\mu_\star = 10^2$ m^2 s^{-1}	$a = 0.01$	$C_{\mathrm{D}} = 1 \cdot 10^{-3}$
$\phi \sim 1^\circ$		

Table 2: Quantities and parameter values used in the numerical experiments with variable embayment length. They are representative for the Western Scheldt

as given in eqn. (7) is such that the total time–averaged flux is zero. Using the knowledge of the equilibrium solution in case of the short embayment limit (see Schuttelaars & De Swart (1996)) and standard numerical methods (continuation techniques in slowly varying parameters), equilibrium bed profiles and their corresponding velocity fields, surface elevations and concentration fields for different embayment lenghts, tidal forcing etc. can be obtained.

4 Results

In the following numerical experiment, the embayment length and the strength of the M_4 overtide will be varied while the other parameters have default values. The default values used in the experiments are given in table 2 and are based on parameters obtained from observations in the Western Scheldt estuary (see Van den Berg *et al.* (1990); De Jong (1998)).

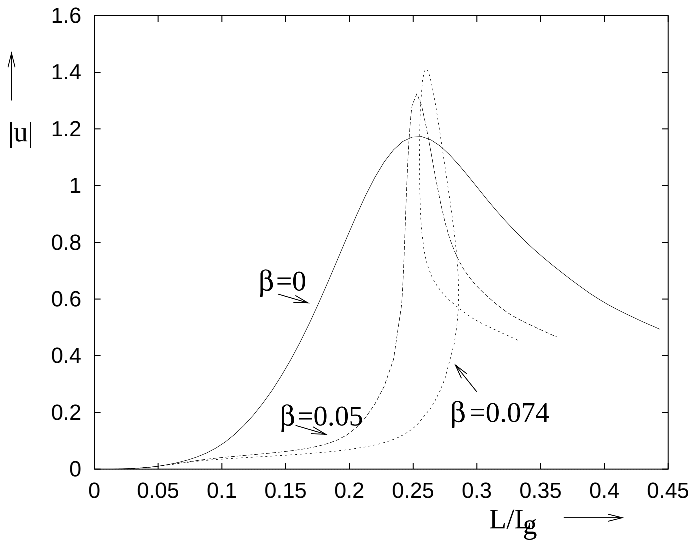

Figure 2: The amplitude of the M_2 horizontal velocity at the entrance of the embayment as a function of the scaled embayment length for different values of β.

In Fig. 2 the dimensionless amplitude of the M_2 horizontal velocity (scaled by $\sqrt{gH}$) at the entrance of the embayment is plotted for different embayment lengths and different values of β, *i.e.*, different strengths of the externally prescribed overtides. First of all it is noted that, although the bed is not flat and friction is important, the resonance length of the embayment *in morphodynamic equilibrium* is approximately $0.25L_g$. In other words there is no shift in the resonance length, as is e.g. found if the friction parameter is increased for a *fixed* bed. Furthermore it is seen that if the externally prescribed overtide is strong enough (see Fig. 2, $\beta = 0.074$), embayment lengths can be found for which more than one morphodynamic equilibrium exists. Note that $\beta \approx 0.074$ for the Western Scheldt.

In general, two different types of equilibria can be distinguished: if the embayment length is smaller than the M_4 friction length scale the bed can become very deep, up to 7 times the depth at the entrance of the embayment (see Fig. 3(a)) Effects of bottom friction are small and the tidal motion has the characteristics of a standing wave, i.e., no phase changes are observed in the embayment (see Fig. 3(b)). Furthermore, it appears that advective fluxes due to internally generated (see Fig. 4(a)) and externally forced overtides (see Fig. 4(b)) make an approximate balance. Since both external and internally generated overtides are important, this equilibrium will be called the *external* equilibrium.

If the length of the embayment becomes larger than the M_4 friction length, the amplitudes of the external M_4 horizontal and vertical tides become very small. The internally generated M_4 tides are much more intense and an approximate balance between the internally generated fluxes is observed (see Figs. 4(c) and 4(d)). In this situation the bottom friction is very significant and the tidal motion has the characteristics of a travelling wave. The maximal bed depth is of the order of twice the depth at the entrance (see Fig. 3). This equilibrium will be called the *frictionally modified* equilibrium.

From Fig. 2 it is now clear what happens if β is increased: if β is small enough the external equilibrium changes gradually into the frictionally modified one. If β is increased, the characteristics of the external equilibrium become more pronounced (for example, the maximum water depth becomes larger if β is increased) and the change towards the frictionally modified equilibrium takes place in a smaller interval of length values. If β is large enough, the two types of equilibria can coexist for the same embayment length, even though their characteristics are completely different. A third equilibrium connects the other two equilibria in a smooth way.

Figure 2 shows that the maximal embayment length decreases with increasing values of β. It can be shown that the maximum embayment length for a given strength of the overtide equals the M_2 frictional length:

$$L_{\mathrm{f}} = \frac{2\pi\sqrt{gh_{\mathrm{min}}H}}{\sigma L}\left[\frac{2}{1+\sqrt{1+\left(\frac{C_{\mathrm{D}}AL}{h_{\mathrm{min}}H^2}\right)^2}}\right]^{\frac{1}{2}} \tag{8}$$

Here h_{min} is a characteristic water depth which depends on the strength of the M_4 overtide. This length scale decreases with increasing values of β through the parameter h_{min}. The theoretical predictions are in good agreement with the full model results. For a derivation, see Schuttelaars (1999).

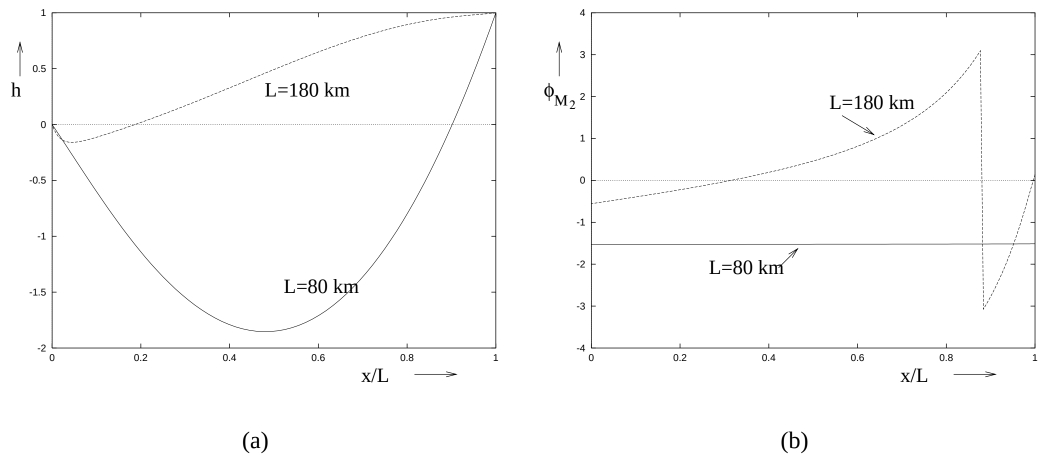

Figure 3: Characteristic bed profiles (figure a) and phase profiles (figure b) for both the external ($L = 80\,\mathrm{km}$) and frictionally modified ($L = 180\,\mathrm{km}$) equilibrium. Here $\beta = 0.074$, the other parameters have the default values.

5 Conclusions

In this contribution an idealized one–dimensional model has been analyzed to gain more understanding of the morphodynamics in long embayments. If the embayment length is much smaller than the tidal wavelength, the momentum equation describes in leading order a pumping mode, if the length is increased, both resonance effects and bottom friction become more important.

Sediment is transported as suspended load, both due to diffusive and advective processes. For a short embayment, the diffusive transport mechanism is most important. However, if the channel length is increased, diffusion becomes less effective and advection is the main transport mechanism. The latter is due to both external and internally generated overtides.

The main aim in this paper was to investigate the possible existence of equilibria. A system is said to be in morphodynamic equilibrium when the averaged sediment flux vanishes throughout the embayment. The water motions in the embayment are forced by externally prescribed M_2 and M_4–tides. Furthermore overtides were generated internally. Using the knowledge of the short embayment limit and numerical continuation techniques, it was shown that equilibrium profiles exist for embayment lengths smaller than the M_2 frictional length. Embayments longer than M_2 frictional length tend to fill up until the maximum embayment length is reached. It was observed that the embayment became resonant for a length of approximately 0.25 times the gravitational wave length. It is well known that the resonance length L_{res} of a frictionless embayment with a flat bottom is 0.25 times the gravitational wave length. An important finding here is that this value is maintained even in a frictional domain due to adjustments of the bottom. Furthermore, it was shown that character of the tidal wave changed from a standing wave character towards a running wave.

If the amplitude of the externally prescribed M_4–tide is large enough compared to the amplitude of the M_2–tide, multiple equilibria can be found. This means that for the

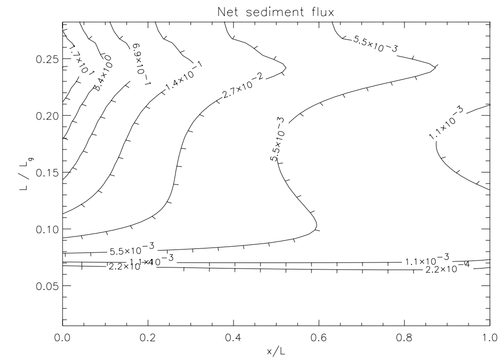

(a) Net sediment flux due to the advective contribution $u^{\mathrm{s}}C^{\mathrm{s}}$.

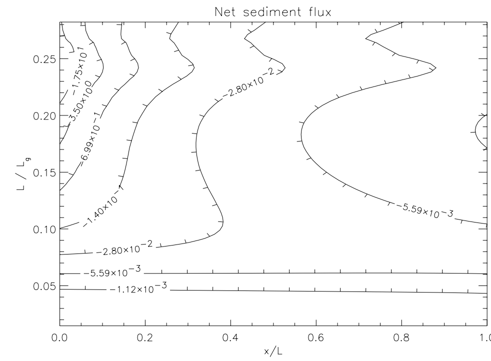

(b) Net sediment flux due to the advective contribution $u^{0}C^{0}$.

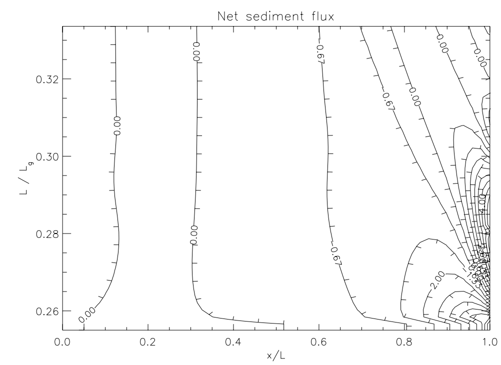

(c) Net sediment flux due to the advective contribution $u^{\mathrm{s}}C^{\mathrm{s}}$.

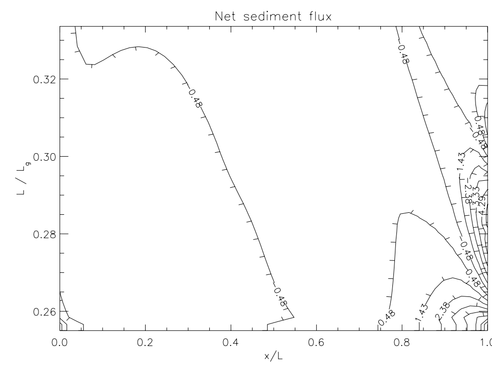

(d) Net sediment flux due to the advective contribution $u^{\mathrm{c}}C^{\mathrm{c}}$.

Figure 4: Contour plots of the leading order sediment fluxes as function of the scaled embayment length L/L_{g} and x/L. Here $L_{\mathrm{g}} = 2\pi\sqrt{gH}/\sigma \sim 550\,\mathrm{km}$ and $\beta = 0.074$. The upper two figures show the largest fluxes for the external equilibrium, the lower two figures those of the frictionally modified equilibrium. The amplitudes of the fluxes are scaled with $(\alpha/\gamma)\,\left(\epsilon\sqrt{gH}\right)^3$. Here $\beta = 0.074$, the other parameters have the default values.

same parameter values more than one morphodynamic equilibrium bed profile exists. These bed profiles have totally different characteristics and may have large practical consequences. For example interferences in an estuary with multiple equilibria may lead to sudden geometrical changes and different tidal characteristics.

At the moment the stability of these morphodynamic equilibria is under study. First results indicate that the external and frictional modified equilibrium are stable and that the intermediate one is unstable. Until now we only focussed on the influence of the ratio of the amplitudes of the externally prescribed tides on the morphodynamic equilibria. A next step would be to investigate the sensitivity on other external parameters and the global stability of these equilibria in more detail. Furthermore, a comparison with field data should be made.

References

CSANADY, G. T. 1982. *Circulation in the coastal ocean*. Dordrecht: Reidel.

DE JONG, K. 1998. *Tidally averaged transport models*. Ph.D. thesis, Delft University of Technology.

DE VRIEND, H. J. 1996. Mathematical modelling of meso–tidal barrier island coasts. Part I: Empirical and Semi–Emperical Models. *Pages 115–149 of:* LIU, P.L.-F (ed), *Advances in coastal and ocean engineering*. World Scientific, Singapore.

FRIEDRICHS, C. T. 1995. Stability shear stress and equilibrium cross–sectional geometry of sheltered tidal channels. *J. Coastal Res.*, **11**, 1062–1074.

LORENTZ, H. A. 1922. Het in rekening brengen van den weerstand bij schommelende vloeistofbewegingen. *De Ingenieur*, 695.

SCHUTTELAARS, H.M. 1997. *Evolution and stability analysis of bottom patterns in tidal embayments*. Ph.D. thesis, University of Utrecht, The Netherlands.

SCHUTTELAARS, H.M. 1999. *One–dimensional long–term equilibria of tidal embayments*. report R99–2. IMAU.

SCHUTTELAARS, H.M. to appear. Long–term modeling of channels and shoals in tidal embayments. PECS 1998.

SCHUTTELAARS, H.M., & DE SWART, H.E. 1996. An idealized long–term morphodynamic model of a tidal embayment. *Eur. J. Mech., B/Fluids*, **15**(1), 55–80.

VAN DEN BERG, J.H., JEUKEN, C.J.L., & VAN DER SPEK, A.J.F. 1990. Hydraulic processes affecting the morphology and evolution of Westerschelde estuary. *Pages 157–184 of:* NORDSTROM, K.F., & ROMAN, C.T. (eds), *Estuarine shores: Evolution, Environments and Human Alterations*. Chisester: John Wiley and Sons Ltd.

VAN DER SPEK, A.J. 1997. Tidal asymmetry and long–term evolution of Holocene tidal basins in The Netherlands, simulation of paleo–tides in the Schelde estuary. *Marine Geology*, **141**, 71–90.

VAN RIJN, L. C. 1993. *Principles of sediment transport in rivers, estuaries and coastal seas*. Amsterdam: Aqua Publ.

VERBEEK, H., TANK, F.T.G., & GROENEWOUD, M.D. 1998. *Drempels in de Westerschelde, natuur en mens samen aan het werk*. Tech. rept. RIKZ.

ZIMMERMAN, J. T. F. 1982. On the Lorentz linearization of a quadratically damped forced oscillator. *Phys. Lett.*, **89A**, 123–124.

ZIMMERMAN, J. T. F. 1992. On the Lorentz linearization of a nonlinearly damped tidal Helmholtz oscillator. *Proc. Kon. Ned. Akad. v. Wetensch.*, **95**, 127–145.